

DYNAMIC SEISMIC TESTING OF LARGE SIZE STEEL DECK DIAPHRAGM FOR LOW-RISE BUILDING APPLICATIONS

R. Tremblay¹, C. Rogers², C.-P. Lamarche³, C. Nedisan³, J. Franquet⁴, R. Massarelli⁵,
and K. Shrestha⁴

¹ Professor, ³ Graduate Research Assistant, Dept. of Civil Geological and Mining Engineering,
Ecole Polytechnique of Montreal, Montreal, Canada

² Associate Professor, ⁴ Graduate Research Assistant, ⁵ Undergraduate Research Assistant,
Dept. of Civil Engineering and Applied Mechanics, McGill University, Montreal, Canada
Email: robert.tremblay@polymtl.ca

ABSTRACT :

A test program was carried out on 21.02 m x 7.31 m metal roof deck diaphragm specimens subjected to dynamically applied in-plane loading. The tests were conducted at different amplitudes of loading: low amplitude vibrations to characterize the dynamic properties of the specimens, variable amplitude excitations to evaluate the change in dynamic properties from elastic response up to yielding, and extreme seismic loading to examine the inelastic cyclic response. Three series of tests were performed: two on new steel roof deck assemblies and one on the first specimen that was repaired after being subjected to the extreme seismic loading condition. The diaphragm stiffness and fundamental period were found to vary significantly with the amplitude of the applied motion. Damage under the extreme loading condition concentrated at the fastener locations, which resulted in pinched hysteretic response and strength degradation. The tests showed that the original in-plane strength and stiffness of metal deck diaphragms could be restored if properly repaired, even after having sustained significant inelastic demand as was applied in the tests.

KEYWORDS: Diaphragm, Period, Pinching, Shear deformations, Shear stiffness, Steel deck

1. INTRODUCTION

Corrugated steel roof decks are commonly used in North America to carry gravity and lateral loads in single-storey buildings. When connected to each other and to the supporting steel, the steel deck sheets form a horizontal diaphragm at the roof level to resist and transfer lateral loads to the vertical bracing system located along the walls of the building (Fig. 1a). These lateral loads are transferred by means of a shearing action, which is reliant on the in-plane shear capacity and stiffness of the deck panels and their connections.

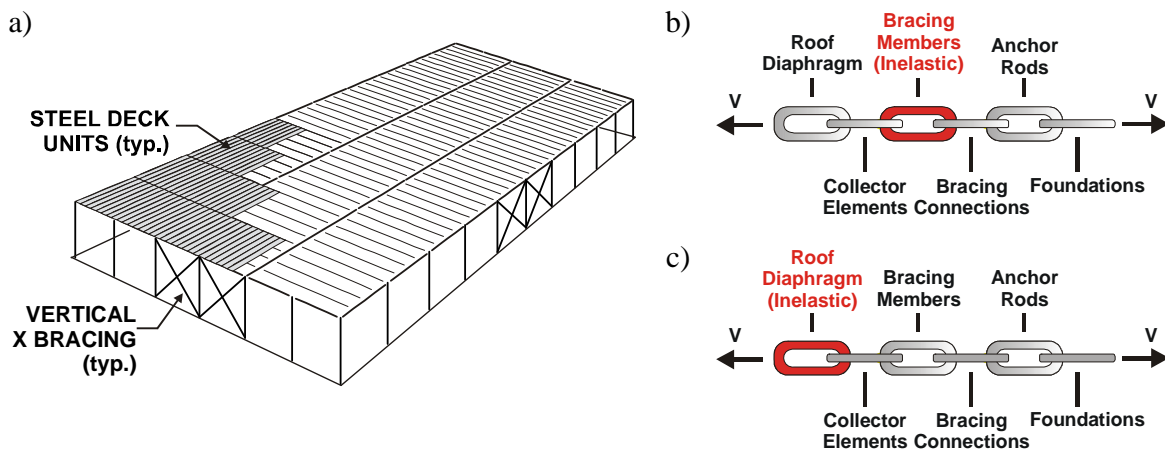


Figure 1 a) Typical single-storey steel building structure; b) Weak brace design; and c) Weak diaphragm design.

The roof deck diaphragm is an integral part of the seismic force resisting system (SFRS), along with the collector and chord members along the roof perimeter, the diagonal bracing members, the brace connections, the anchor rods, and the foundations. Tremblay and Rogers (2005) investigated two different seismic design methods that incorporate the roof deck diaphragm. The current approach to design is to specify the braces to act as the weak, or fuse elements, which dissipate the energy input from the earthquake through inelastic buckling and tensile yielding. The roof diaphragm and other elements in the SFRS are selected to carry the probable capacity of the fuse (Fig. 1b). This often results in much thicker decks and substantially more diaphragm connections than used in past practice due to the overstrength of the braces, especially when initially designed as a tension-compression bracing system. An alternate design procedure is to consider the roof diaphragm as the fuse in the SFRS (Fig. 1c). This could potentially decrease building costs because the overstrength of the diaphragm is minimal; thus the probable capacity used in the selection of the elements in the SFRS would be less than that associated with the common approach to design in Fig. 1b. To further improve upon the seismic design approach, the in-plane flexibility of the diaphragm could also be accounted for to increase the overall period of vibration of the building. This could result in decreased seismic design forces as calculated using the relevant building code and an overall reduction in cost of the structure. Small-scale diaphragm tests and analytical building models have been run to evaluate these two possible design procedures. Analytical studies have shown that the period of vibration of a single-storey building with a flexible roof diaphragm may be longer than that based on the stiffness of the vertical bracing system alone, which can result in significant reductions in seismic design forces (Tremblay et al., 2002). Recent studies showed however that building periods based on low amplitude ambient vibration tests are generally much shorter than those obtained from analytical predictions (Lamarche, 2005). Tremblay et al. (2008) also carried out ambient vibration tests of a building and compared the results to the period values predicted from a numerical model of a typical single-storey building with a flexible metal roof deck diaphragm.

Given these background studies two general objectives led to the need to carry out the dynamic testing of roof deck diaphragms: i) to develop methods to more accurately predict the period of vibration of single-storey buildings for the determination of the seismic loads while accounting for roof diaphragm flexibility, and ii) to develop seismic design guidelines and detailing provisions to take advantage of the flexibility and ductility of the roof diaphragm in seismic design. This paper describes a test program that has been conducted on two large size diaphragm specimens to achieve these objectives. The tests were carried out under different dynamic loading signals at various amplitudes. Elastic and inelastic diaphragm responses are investigated. For one specimen, the test series was repeated on the diaphragm that had been repaired after being subjected to dynamic loading in the inelastic range. Comparisons between test results and numerical predictions are also presented and discussed.

2. TEST PROGRAM

2.1 Test Setup

The test setup consisted of the horizontal rectangular 7.31 m x 21.02 m steel deck diaphragm shown in Fig. 2a. The test frame was composed of the components typically found in the roof of a building, including regularly spaced open web steel joists and perimeter W-section beams. In the test program described herein, the deck sheets were laid out on the steel joists, parallel to the long side. The steel joists were designed with top chord members and overall depth dimensions (600 mm) that are typically found in medium to long span applications. The joists also had end seats, 100 mm deep, for direct support on the top flange of the W360x39 beams running along the long edges. Shear force transfer between the steel deck diaphragm and these beams was done through shear connectors made of square tubing segments that were welded to the beams between the joist seats. At the two ends of the test frame, the deck sheets were directly fastened to the W360x39 edge beams. All perimeter beams were detailed so that they could be flipped upside down when using the frame for testing diaphragms with joists and deck sheets oriented in the direction perpendicular to the one shown in Fig. 2.

Instead of columns, the frame was supported on rockers to allow for lateral movement parallel to the short dimension. Dynamic excitation along this direction was applied at each end of the frame using two identical 1000 kN high performance dynamic actuators acting in phase. In the tests, inertia forces were induced along the length of the diaphragm due to the self-weight of the steel deck-frame assembly. Additional weight was introduced to represent the mass that would be present in the roof of a building from non-structural components: 576 steel bars were uniformly distributed over the steel deck area (Fig. 2b) and pairs of steel plates welded on both sides of the open web steel joists (Fig. 2a). The total weight of the test specimen was 120 kN: deck sheets (13.0 kN), steel bars on deck (34.1 kN), steel joists plus added plates (13.7 + 29.3 = 43.0 kN), transverse beams (20.2 kN), and parallel beams (9.7 kN). As illustrated in Fig. 2c, extensive instrumentation was implemented to capture the response of the specimens. In particular, accelerometers and displacement transducers were used at very other joist location along the span of the diaphragm, and slip at side-lap connections was monitored at mid-length of the exterior deck sheets.

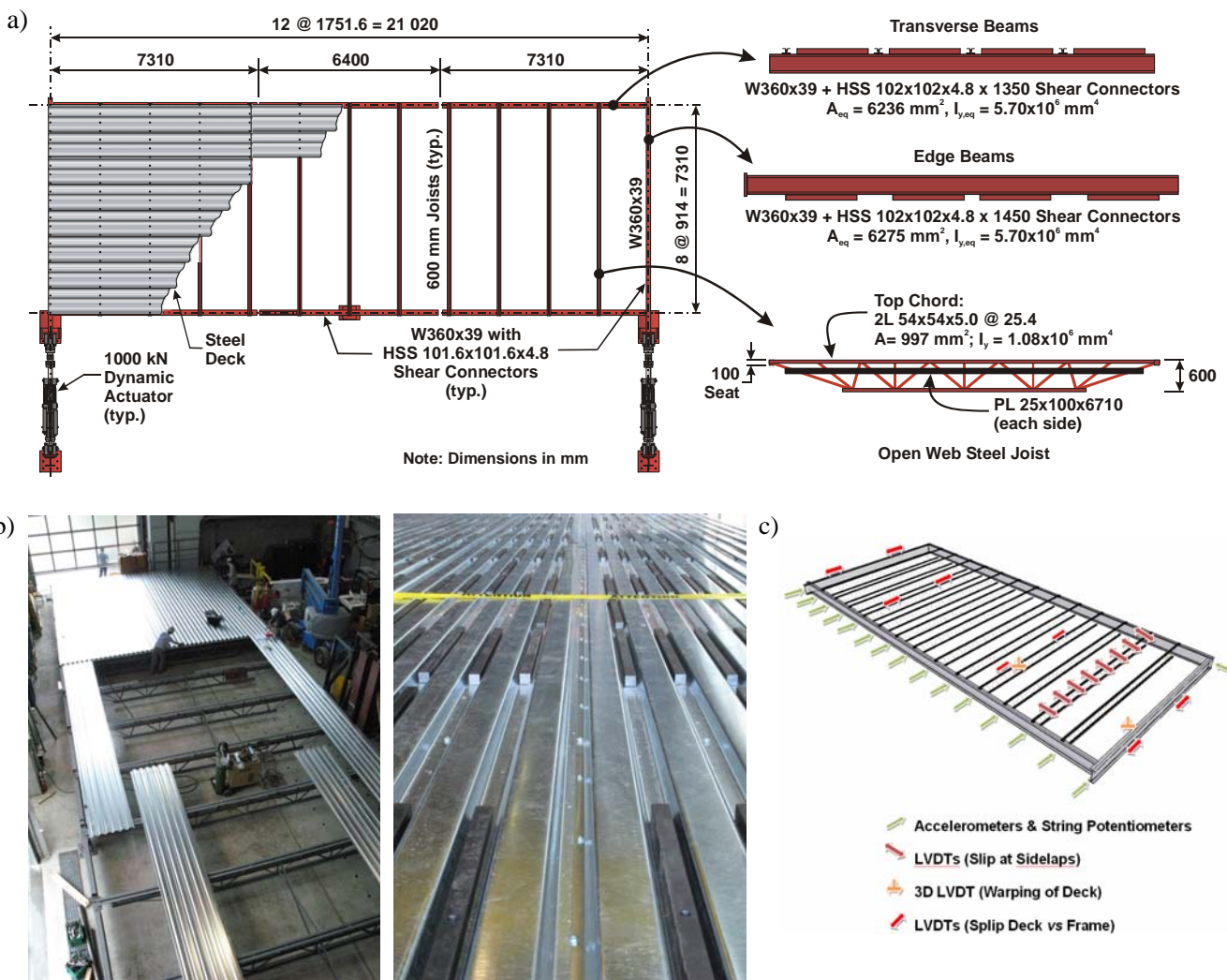


Figure 2 Test setup: a) Plan view and detail of the perimeter beams and steel joists; b) Photos during assembly and after installation of the deck and additional steel bars; and c) Instrumentation.

2.2 Test Specimens

The test specimens were made of 38 mm deep x 914 mm wide, P3606 Canam nestable steel deck sheets. The deck has a trapezoidal profile with flutes spaced at 152 mm o/c (Fig. 3a). They are made of 0.76 mm thick, Z275

(G90) galvanized steel complying to ASTM A653, grade SS with nominal yield strength $F_y = 230$ MPa and tensile stress $F_u = 310$ MPa. Each test specimen comprised a total of 24 sheets: 3 over the length x 8 over the width. The sheets were connected to the steel joist top chords and to the shear connectors on the transverse beams using Hilti X-EDNK22-THQ12M powder-driven fasteners arranged on a 914/4 pattern (one fastener at every other flute). Hilti X-EDN19-THQ12 powder-driven fasteners were used on the same pattern along the edge beams parallel to loading. Side-lap connection was made with 5 Hilti S-MD 12-14x1 (#12) self drilling screws between each joist. Two specimens were tested: DIA-1 and DIA-2. The difference between the two diaphragms was that there was no overlap at the end joints of the panels in specimen DIA-2 (Fig. 3b) whereas the sheets in specimen DIA-1 were overlapped 50 mm. This allowed for a quantitative measurement of the effect on stiffness contribution due to the restraint of warping at the overlap location.

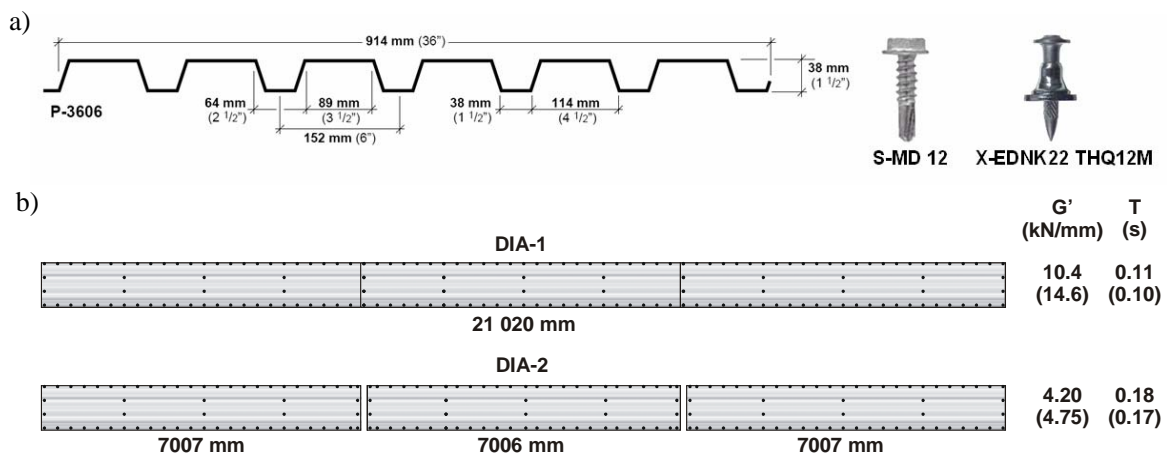


Figure 3 a) Steel deck profile and connectors; b) Steel sheet arrangements with predicted stiffness and periods.

The strength and stiffness of the diaphragm assemblies were determined using the SDI method (Luttrell, 2004) assuming the nominal strength (Q) and flexibility (S) properties of the connectors for 0.76 mm thick steel: $Q_f = 6.71$ kN, $S_f = 0.0413$ mm/kN for the structural connectors and $Q_s = 3.23$ kN and $S_s = 0.099$ mm/kN for the side-lap connectors. With these assumptions, the diaphragm shear strength, q_u , is equal to 13.0 kN/m. It is governed by failure of the corner fasteners and is not influenced by the end lap joint condition. Failure of the fasteners of intermediate panels would occur under a shear force of 14.2 kN/m. In the SDI method, the determination of the shear stiffness, G' , accounts for several parameters including distortion (warping) of the deck sheets at their ends and the flexibility of the connectors. G' takes a value of 4.2 kN/mm assuming individual sheet response. In DIA-1, warping deformations are restrained at the two intermediate overlapped joints and G' increases to 10.4 kN/mm if the full sheet length of 21.02 m is considered in the calculations (Fig. 3b). Connector flexibility effects on G' are discussed later.

2.3 Test Program

Four types of tests were conducted sequentially on each diaphragm specimen. First, tests under ambient vibration and low amplitude white noise signals were completed to determine the natural frequency of the diaphragm at various cyclic amplitudes. These were followed by sine sweep tests at sequential frequencies and variable amplitude excitations, still in the diaphragm's elastic mode, to obtain further data on the influence of loading amplitude on stiffness and period. Seismic signal SS1 was applied in the third type of tests. This signal is an acceleration record from the 1989 Loma Prieta earthquake (Stanford Univ. 360°) with a peak value of 0.29 g. A time scale factor of 1/3 was used to reflect the difference between the fundamental period of the test specimens and that of actual low-rise buildings. Several tests were performed in the elastic range by varying the amplitude of the SS1 signal from 40% to 160%. Lastly, two tests were performed using a sinusoidal harmonic signal (SS2) with a frequency of 4.0 Hz, a peak displacement of 30 mm (peak acceleration of 1.93 g) and a total duration of 10 s. The signal has a linear rise time of 2.5 s (8 cycles) and a linear descending branch of 5.5 s (16 cycles). The

signal was applied twice, at 5% and 80% of its full amplitude. The 0.80 x SS2 signal was expected to induce inelastic response and structural damage and, hence, was applied last. After application of the entire test program on specimen DIA-1, the diaphragm was repaired by installing new structural and side-lap connectors at every location where damage was visible. The repaired specimen, referred to as DIA-1R, was then subjected to the entire test program before it was removed and replaced by specimen DIA-2.

3. NUMERICAL SIMULATIONS

The fundamental period, T , of a rectangular diaphragm with uniform mass and stiffness properties and lateral supports at both ends can be determined analytically, as illustrated in Fig. 4a (Medhekar, 1997; Tremblay et al., 2000). In this expression, W is the total seismic weight, K_D is the equivalent stiffness of the diaphragm, including in-plane flexural and shear deformations (Δ_F & Δ_W), g is the acceleration due to gravity ($g = 9810 \text{ mm/s}^2$), L and b are respectively the diaphragm span and depth, EI is the flexural stiffness of the diaphragm, as provided by the transverse edge members, and G' is the diaphragm shear stiffness. For the test specimens, $W = 110 \text{ kN}$ (excluding the edge beams parallel to loading), $L = 21020 \text{ mm}$, $b = 7310 \text{ mm}$, and $EI = 167 \times 10^9 \text{ mm}^4$. Using $G' = 4.20 \text{ kN/mm}$, the period $T = 0.18 \text{ s}$. If G' is taken equal to 10.4 kN/mm (Specimen DIA-1 in Fig. 2b), T reduces to 0.11 s .

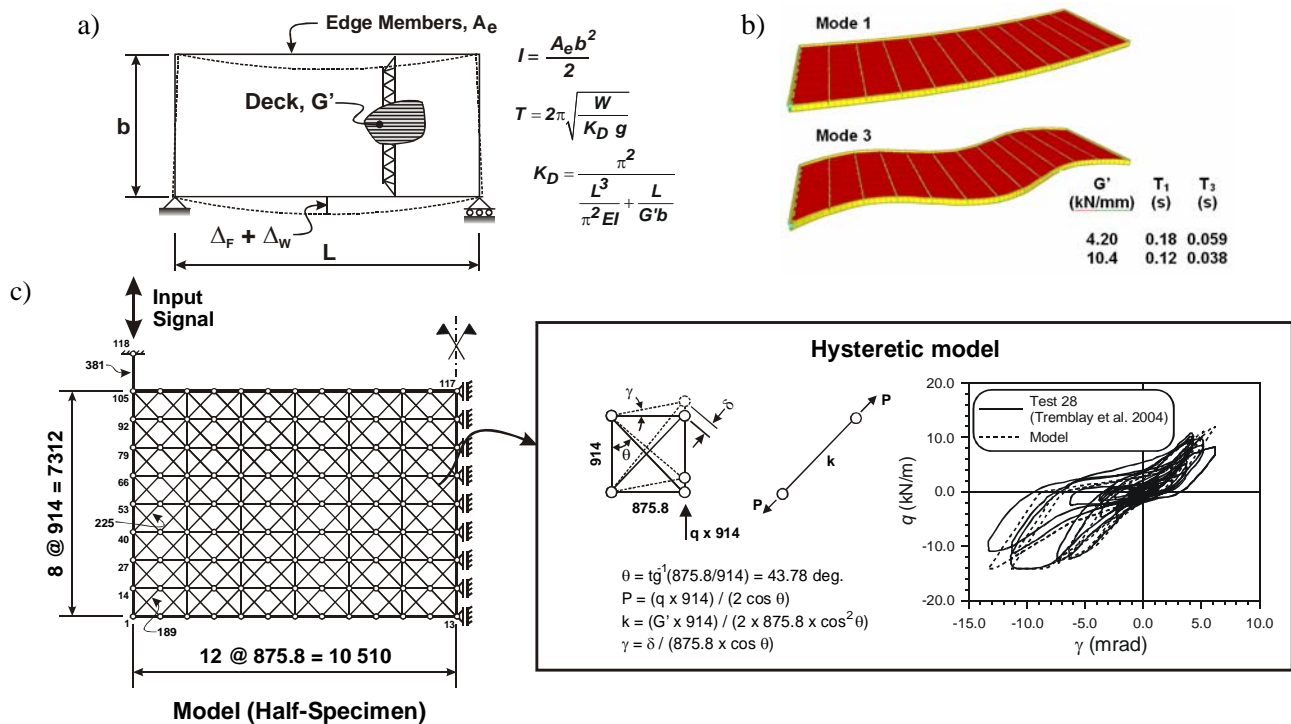


Figure 4 Diaphragm models: a) Fundamental period for a uniform rectangular diaphragm; b) SAP2000 model of the test specimens (1st and 3rd vibration modes shown); and c) Ruaumoko nonlinear equivalent truss model.

Alternatively, numerical models can be used to estimate the dynamic properties of the test specimens. A simple finite element model that includes beam and shell elements was built using the SAP2000 program (CSI, 2005). The shell elements are assigned the steel material properties ($E = 200\,000 \text{ MPa}$, $G = 77\,000 \text{ MPa}$) and the sheet steel thickness (0.76 mm). Using the property/stiffness modifier feature of the program, a membrane shear (f_{12}) modifier is specified such that the product $G \cdot t = G'$ (e.g., $\times 0.0718$ to obtain $G' = 4.20 \text{ kN/mm}$). Membrane f_{11} and f_{22} modifiers were set to 1.33 and 0.05 to reflect the actual in-plane axial stiffness of the deck sheets in their axial and transverse directions, respectively. Figure 4b shows the 1st and 3rd in-plane vibration modes of the test specimens, corresponding to the first two modes to be excited by identical and synchronized signals applied at

both ends of the test frame. The periods computed with the two G' values correspond well to those obtained from the simple analytical expression of Fig. 4a. The SAP2000 model can also be used to predict the elastic dynamic response under various dynamic signals. For instance, specifying 2% Rayleigh damping in the 1st and 3rd modes, the unit shear force reaches a peak value of $0.6 q_u$ under $1.6 \times SS1$ and $1.6 q_u$ under $0.8 \times SS2$ when $G' = 4.2 \text{ kN/mm}$ is assumed. Hence, the diaphragms were expected to remain elastic under $1.6 \times SS1$ whereas the tests with $0.8 \times SS2$ would push the deck in the inelastic range as would be the case for a structure designed with a ductility related factor of 1.6. If $G' = 10.4 \text{ kN/mm}$ is used in the analysis, the corresponding shear demand values are respectively 0.77 and $1.11 q_u$. These significant changes in response reinforce the importance of properly determining the diaphragm G' and T properties in order to adequately predict the seismic demand.

Figure 3c shows a third model that was developed to predict the inelastic seismic response of the test specimens. This model was built with the Ruaumoko computer program (Carr 2004) and is similar to the one used by Tremblay and Rogers (2005) in their study of building structures with inelastic diaphragms. Diagonal truss elements are used to mimic the shear response of the deck. These elements are assigned a Wayne-Stewart axial hysteretic behaviour with stiffness degradation and pinching. The initial stiffness and ultimate strength of the elements were set to respectively correspond to the diaphragm G' and q_u values. Other parameters were calibrated based on tests performed on similar diaphragm specimens (Tremblay et al. 2004). Horizontal elastic truss elements are also introduced in the Ruaumoko model to account for in-plane axial and transverse stiffness of the deck sheets. The perimeter beams and joist top chords are also modeled with beam elements. The model yields the same period estimates and elastic response predictions as the SAP2000 model.

4. RESULTS

4.1 Fundamental Period of Vibration

Values of the fundamental period obtained from white noise and sine sweep tests are plotted in Fig. 5a. In all cases, the period is found to increase when increasing the level of excitation. For specimens DIA-1 and DIA-2, the variation at low amplitude is more pronounced. Relative movements in the connections are locked up at low amplitude, which results in overall higher stiffness and shorter periods. If the flexibility of the deck connectors is omitted in the SDI procedure, G' increases to the values in brackets in Fig. 3.2b. For specimen DIA-1, the corresponding period (0.10 s) agrees well with the measured periods at low amplitude (0.11 s). For Specimen DIA2, the predicted value of 0.17 s is longer than what was measured (0.13 s). Once relative movement is mobilized between the components, the period keeps increasing with load amplitude, but at a smaller pace. Warping restraint due to the overlapped end joints in Specimen DIA-1 resulted in shorter periods compared with Specimen DIA-2. For both specimens, the periods measured under high amplitude motions exceeded the predictions based on SDI G' values. For instance, T for Specimen DIA-2 tends towards a value of 0.25 s. For this

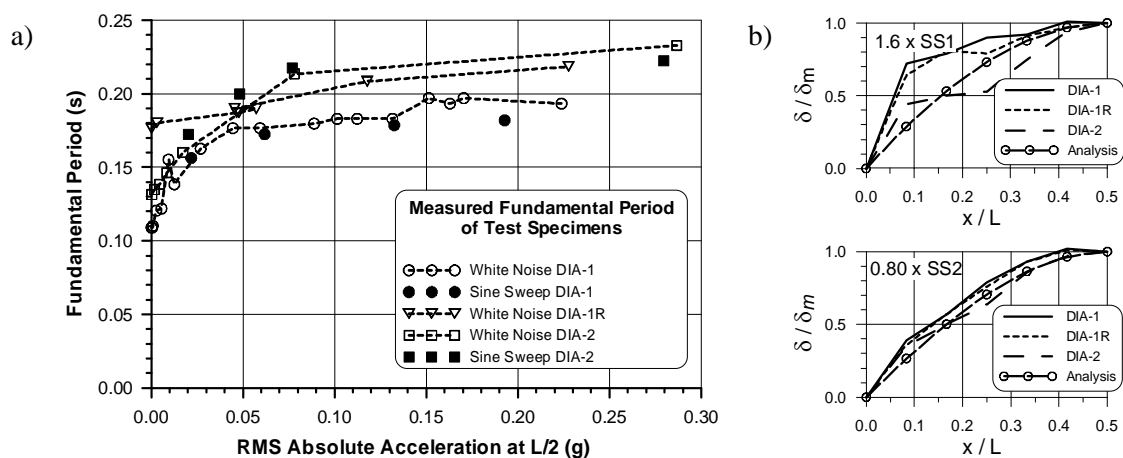


Figure 5 a) Fundamental period from tests; b) End shear-mid-span deflection hysteretic response under $1.6 \times SS1$, $0.05 \times SS2$ and $0.80 \times SS2$ of specimens: a) DIA-1; b) DIA-1R; and DIA-2.

to occur, G' must be reduced to 2.1 kN/mm, which is half the SDI prediction assuming individual sheet response, and 20% of the value predicted assuming no warping distortion at the end joint overlaps. This suggests that the SDI method may overestimate the shear stiffness for this type of diaphragm when subjected to cyclic dynamic loading. For Specimen DIA-1R, the repair strategy after strong shaking in the inelastic range permitted the recovery of near the original in-plane stiffness of Specimen DIA-1, except in the very low amplitude range.

4.2 Seismic Response

Figure 6 shows the end shear (q) vs diaphragm mid-span deflection (δ_m) hysteretic response of the three diaphragms under 0.8 times the SS2 signal. In all three tests, the specimens reached the predicted ultimate shear strength, q_u , and experienced similar level of inelastic deformations. Damage concentrated at the fasteners of the end sheets with tilting of the side-lap screws and deck bearing failure against the structural connectors. The response of all specimens is characterised by gradual pinching due to loosening of the connectors and strength degradation in the large inelastic excursions. Adding new fasteners at locations where damage occurred under strong seismic demand could bring the shear strength back to its original level (DIA-1R vs DIA-1). As expected, the end lap condition had no significant effect on the strength of the diaphragms (DIA-2 vs DIA-1), although it influenced the deformed shape under elastic response. Figure 5b compares the envelope of in-plane deformations along the diaphragm span under 1.6 times the SS1 signal and 0.8 times the SS2 signal. Under 1.6 x SS1, specimens DIA-1 and DIA-1R exhibited relatively higher deformations near the ends of the test frame, a phenomenon that was not observed in the other tests and in the elastic analysis. Figure 7 shows the time history of the mid-span deflection, δ_m , and the hysteretic response of specimen DIA-2 under 1.6 x SS1 and 0.8 x SS2 signals. The results from the Ruaumoko analyses are also plotted in the figure. Good agreement, both in phase and amplitude, was obtained when specifying $G' = 2.1$ kN/mm ($T = 2.5$ s) in the numerical model. The hysteretic response was also well predicted in both tests, including pinching under the stronger signal. Strength degradation could not be reproduced in this study and refinement of the model is needed to properly simulate inelastic response.

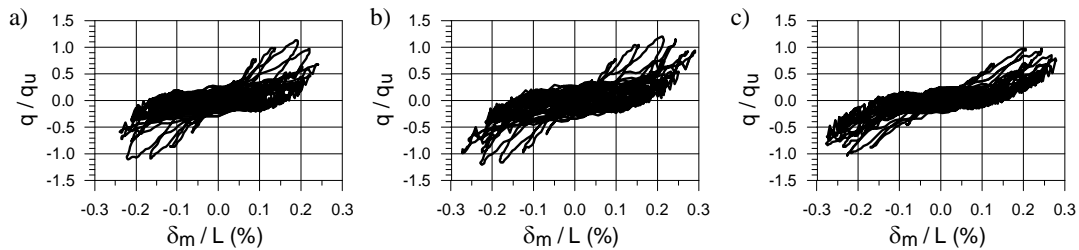


Figure 6 Shear-deflection hysteretic response under 0.80 x SS2 for: a) DIA-1; b) DIA-1R; and c) DIA-2.

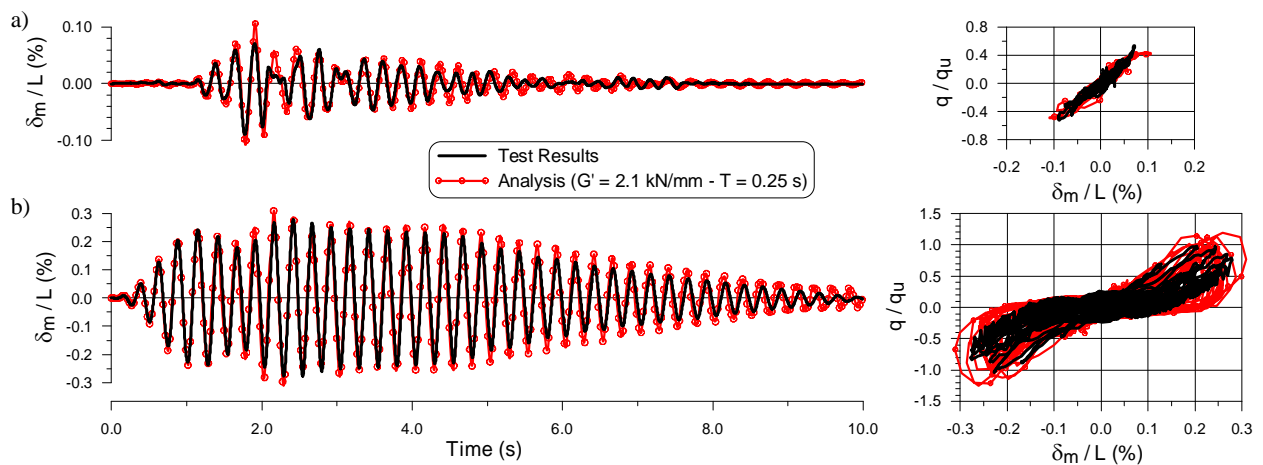


Figure 7 Time history and hysteretic responses of specimen DIA-2 under: a) 1.6 x SS1; b) 0.80 x SS2.

5. CONCLUSIONS

Dynamic seismic tests were carried out on two large scale metal roof deck diaphragm specimens made of 0.76 mm thick steel deck sheets. Self-drilling side-lap screws and powder-driven structural connectors on a 914/4 pattern were used in the tests. The stiffness and fundamental period of the diaphragms varied significantly with the amplitude of dynamic loading. For the specimen without overlapped end joints, the SDI shear stiffness assuming individual sheet response led to period estimates that were longer than the values obtained under small vibrations but shorter than the periods measured under stronger shaking. The use of overlapping end joints shortened the periods but the predictions under strong shaking remained lower than the measurements. The test shear resistance of both specimens agreed very well with the SDI nominal values. Overlapping end joints had no noticeable effect on the diaphragm strength. Metal roof decks loaded beyond their shear capacity experienced damage localised at the side-lap and structural connectors of the end sheets, where the shear demand was higher. The experiments showed that it was possible to restore the original stiffness and strength of a damaged diaphragm so that it could resist another earthquake. Further testing is needed to examine the influence of sheet steel thickness and connector designs. The fundamental period of vibration and overall elastic and inelastic responses to dynamic excitations of the test specimens could be well predicted using numerical models, provided that the diaphragm shear stiffness was known. End lap joint effects on elastic response should be investigated further in future numerical studies. More refined numerical models are also needed to predict diaphragm strength degradation and quantitatively assess the damage to individual fasteners under inelastic seismic loading.

ACKNOWLEDGEMENTS

Funding for this research was provided by the Natural Sciences and Engineering Research Council of Canada, the Vancouver Steel Deck Diaphragm Design Committee (VSDDC), WSB Consulting Structural Engineers, RJC Consulting Engineers, the Canadian Sheet Steel Building Institute, the Steel Deck Institute, and Hilti Canada. Material for the test frame was donated by Sofab Structural Steel Inc. and the Canam Group. The Canam Group also supplied the deck material and Hilti Canada Inc. donated the deck fasteners. The authors also wish to express their appreciation for the most valuable technical input from the industrial partners.

REFERENCES

- Carr, A.J. (2004). RUAUMOKO, Inelastic Dynamic Analysis Program. Dept. of Civil Engineering, University of Canterbury, NZ.
- CSI. (2007). SAP 2000 Integrated Software for Structural Analysis & Design, Version 11. Computers and Structures, Inc., Berkeley, CA.
- Lamarche, C.-P. (2005). Étude Expérimentale du comportement dynamique des bâtiments de faible hauteur en acier. M.Sc. Thesis. Dept. of Civ. Eng., Univ. of Sherbrooke, Sherbrooke, QC. (*in French*)
- Luttrell, L. (2004). Diaphragm Design Manual, 3rd ed., Steel Deck Institute, Fox River Grove, IL.
- Medhekar, M.S. (1997). Seismic Evaluation of Steel Buildings with Concentrically Braced Frames. Ph.D. Thesis, Dept. of Civil and Environmental Eng., Univ. of Alberta, Edmonton, AL.
- Tremblay, R., Nedisan, C.D., Lamarche C.-P., Rogers, C.A. (2008). Periods of Vibration of a Low-Rise Building with a Flexible Steel Roof Deck Diaphragm. *Proc. 5th Int. Conf. on Thin-Walled Structures*, Brisbane, Australia, 615-622.
- Tremblay, R., Rogers, C.A., (2005) Impact of Capacity Design Provisions and Period Limits on the Seismic Design of Low-Rise Steel Buildings. *Int. J. of Steel Structures*, **5:1**, 1-22.
- Tremblay, R., Rogers, C., Martin, É., and Yang, W. (2004). Analysis, Testing and Design of Steel Roof Deck Diaphragms for Ductile Earthquake Resistance. *J. of Earthquake Eng.*, **8:5**, 775-816.
- Tremblay, R., Rogers, C., and Nedisan, C. (2002). Use of Uniform Hazard Spectrum and Computed Period in the Seismic Design of Single-Storey Steel Structures. *Proc. 7th U.S. Nat. Conf. on Earthquake Eng.*, Boston, MA, Paper No. 195.
- Tremblay, R., Berair, T., and Filiatrault, A. (2000). Experimental Behaviour of Low-Rise Steel Buildings with Flexible Roof Diaphragms. *Proc. 12th World Conf. on Earthquake Eng.*, Auckland, NZ, Paper No. 2567.